ISSN: 2640-5571

Research Article

Advances in Nanoscience and Nanotechnology

# Experimental Evaluation of Kinetic Characteristics of SiO2@AuNPs Nanocomposite and BSA-stabilized gold Nanoparticles toward Peroxidase-Mediated Reactions

**Saeed Reza Hormozi Jangi[1]***

*Hormozi Laboratory of Chemistry and Biochemistry, Zabol, 9861334367, Iran.*

***Corresponding Author**
Saeed Reza Hormozi Jangi, Hormozi Laboratory of Chemistry and Biochemistry, Zabol, 9861334367, Iran.

**Submitted:** 2023, Sep 05; **Accepted:** 2023, Sep 25; **Published:** 2023, Sep 30

**Citation:** Hormozi Jangi, S. R. (2023). Experimental Evaluation of Kinetic Characteristics of SiO2@AuNPs Nanocomposite and BSA-stabilized gold Nanoparticles toward Peroxidase-Mediated Reactions. *Adv Nanoscie Nanotec, 7*(1), 01-11.

**Abstract**

*In this study, BSA-stabilized gold nanoparticles and $SiO_2$@AuNPs nanocomposite were synthesized and then characterized by the TEM imaging method. The average size of BSA-stabilized gold nanoparticles was found to be as small as 13 nm while the $SiO_2$@AuNPs nanocomposite showed a mean size of 204 nm. The experimental studies revealed that both BSA-stabilized gold nanoparticles and $SiO_2$@AuNPs nanocomposite exhibit intrinsic peroxidase-like activity. Hence, to explore more precise no their catalytic efficiency and substrate affinity of them, the kinetic characteristics of both nanozymes were quantified using the Menten kinetic model, and the provided results were compared. Upon using TMB as peroxidase substrate, $V_{max}$ of 0.022 µM $min^{-1}$ and a Km of 0.06 mM for the $SiO_2$@AuNPs nanocomposite was achieved while for the BSA-stabilized gold nanoparticles, a $V_{max}$ and $K_m$ at about 0.263 µM $min^{-1}$and 0.03 mM, in order, was estimated. The $V_{max}$ of BSA-stabilized gold nanoparticles was 12.0-fold higher than that of $SiO_2$@AuNPs nanocomposite, revealing that the catalytic efficiency of BSA-stabilized gold nanoparticles is 12.0-fold higher than $SiO_2$@AuNPs nanocomposite. Besides, the $K_m$ value of $SiO_2$@AuNPs nanocomposite was 2-order higher than that of BSA-stabilized gold nanoparticles, indicating that the substrate affinity toward BSA-stabilized gold nanoparticles is 2.0-order higher than the $SiO_2$@AuNPs nanocomposite. Since, the active nodes of both nanozymes are same (i.e., gold), the difference between their catalytic efficiency and affinity can be assigned to their different sizes and the ability of the active nodes to bind the substrate. Based on the results of this work, small-size BSA-stabilized gold nanoparticles are characteristically more efficient peroxidase mimic materials than the $SiO_2$@AuNPs nanocomposite.*

**Keywords:** BSA-stabilized gold nanoparticles; $SiO_2$@AuNPs nanocomposite; peroxidase mimics; Kinetics studies; shelf stability

## 1. Introduction

Importance and practical application of nanotechnology in modern life lead to design and synthesis of different nanomaterial's with optical [1-3], catalytic [4, 5], anti-cancer features [6], medical [7], or anti-bacterial [8, 9] characteristics such as carbon and metal-based nanoparticles [10, 11], quantum dots [12, 13], metal oxide nanoparticle [14], magnetic nanoparticles [15], and metal-organic frameworks [16, 17], etc. Among various nanoparticles with different properties, recently, nanomaterial with enzyme-like properties, called nanozymes have been widely utilized for catalyzing industrial, clinical, and environmental enzyme-mediated reactions under harsh conditions [18-21]. The most significant advantage of these nanozymes compared to the native enzymes is their lower cost, higher efficiency, and especially, their high cycling stability and recyclability [19, 22]. Up to now, different nanoparticles with intrinsic peroxidase-like activity were designed and synthesized, for instance, $Mn_3O_4$ nanozymes [23], Cu-$CuFe_2O_4$ nanozymes [24], BSA-stabilized manganese dioxide nanoparticles [25], BSA-stabilized manganese phosphate Nano flower [26] carbon nanozymes [27], silica-coated-magnetic nanoparticles [28], $MnO_2$ nanoparticles [29], $Fe_3O_4$ nanozymes [30], self-cascade pyrite nanozymes [31], metal-organic frameworks [32], gold nanozymes [33], S/N cooped carbon nanozymes [34], and silver nanoparticles [35]. Among the different nanomaterials with excellent peroxidase-like activity, gold-based nanozymes have been widely for developing nanozyme-based sensors [36, 37], nanozyme-based cancer treatment [38], and nanozyme-mediated dye degradation [39]. Moreover, since the first report of patients infected with the new infection disease, COVID-19 in 2019 [40, 41], nanozyme-based methods have been developed for fast clinical diagnosis of this pandemic infection [42]. Hence, evaluation of their biochemical features and enzyme-like properties is important for developing nanozyme-based systems with better figures of merit. In this regard, the biochemical behavior of enzyme-like Nano silver was also investigated by our research group [43]. Besides, recently, our research group reported a research article on the investigation of biochemical behaviors of BSA-stabilized gold nanoparticles [44, 45]. In this study, BSA-stabilized gold nanoparticles and $SiO_2$@AuNPs

nanocomposite were synthesized and then characterized by the TEM imaging method. The experimental studies revealed that both BSA-stabilized gold nanoparticles and $SiO_2$@AuNPs nanocomposite exhibit intrinsic peroxidase-like activity. Hence, to explore more precise no their catalytic efficiency and substrate affinity, the kinetic characteristics of both nanozymes were quantified using the Menten kinetic model, and the provided results were compared. Based on the results of this work, small-size BSA-stabilized gold nanoparticles are characteristically more efficient peroxidase mimic materials than the $SiO_2$@ AuNPs nanocomposite.

## 2. Experimental

### 2.1. Synthesis protocols of nanomaterials

For the synthesis of BSA-stabilized gild nanoparticles, 10.0 mm $HAuCl_4.4H_2O$ (5.0 mL) was introduced to 50 mg $mL^{-1}$ bovine serum albumin (BSA; 5.0 mL), followed by stirring at 37 °C and adding 1.0 M Noah to adjust ph. The solution was incubated at 37 °C for 12 hours to complete the synthesis process.

For synthesis, the $SiO_2$@AuNPs nanocomposite, in a typical experiment, 1.0 mL of HAuCl4, 10.0 all terraces (hydroxymethyl) phosphonium chloride, and 500.0 all Noah (2.0 M) were introduced in 50.0 mL deionized water. The resulting mixture was stirred for about 1.0 hour to prepare the colloidal gold solution. To synthesize the amino-functional $SiO_2$ NPs, 1.5 mL of TEOS was added into 40.0 mL of pure ethanol, followed by the addition of 3.0 mL of $NH_4OH$. The mixture was stirred for about 20.0 hours. Afterward, 20.0 mg of the resulting precipitate was treated with 600.0 all of APTES for preparation of the final product. Afterward, 10.0 mg of the amino-functional $SiO_2$ NPs were incubated with a solution of colloidal gold (prepared in section 2.3) for about 12.0 hours. Afterward, the product was separated from the reaction media upon centrifuge at 10000 rpm for 30.0 min. The resulting product was dispersed in 1 mg mL-1 of PVP (stabilizer) aqueous solution, followed by the addition of 60.0 all of HAuCl4 (10.0 mm) and 120.0 all of 10.0 mm ascorbic acid (reducing agent) into the reaction media. The synthesis process was followed by stirring the above-mentioned mixture for about 5 min. afterward, the resulting $SiO_2$@AuNPs nanocomposite was collected, washed, and then dried at room temperature.

### 2.2. Nanozyme Activity Assay

In a typical assay, 100.0 µL of different concentrations of TMB solution was introduced into 1.0 mL acetate buffer (pH=4.0) containing the $SiO_2$@Au nanocomposite or BSA-stabilized gold nanoparticles, followed by adding 100 µL $H_2O_2$ solution. The reaction mixture was incubated at ambient conditions for about 0.5 hours (for $SiO_2$@Au nanocomposite) and 10.0 min (for BSA-stabilized gold nanoparticles). Afterward, the spectrum of the colored product was recorded over 350.0-700.0 nm for calculating the enzyme-like activity of both nanozymes in µM $sec^{-1}$.

## 3. Results and Discussion

### 3.1. Characterization of BSA-Stabilized Gold Nanoparticles

The as-prepared BSA-stabilized gold-nanozymes were synthesized via a simple, high throughput and green method at physiological temperature and then characterized for their morphological properties and size by the TEM imaging method. The morphological properties and the mean size of the as-prepared nanozymes were investigated by the TEM imaging method. To do this, the TEM image of the as-prepared nanozymes was recorded. The results are shown in Figure 1, as shown in this figure, the as-prepared nanozymes show a semi-spherical morphology with uniform particles. It is mentionable that, the uniformity of the particles of the as-prepared nanozymes is a significant advantage from an enzymatic point of view because the uniform particles showed higher enzyme-like activity than the particles with low uniformity. Besides, the results showed that the as-prepared nanozymes have a narrow size distribution of 7.7-18.3 nm with a mean size of about 13 nm which makes them suitable for enzyme-mimicking applications because the size of nanozymescan strongly affect their enzyme-like activity.

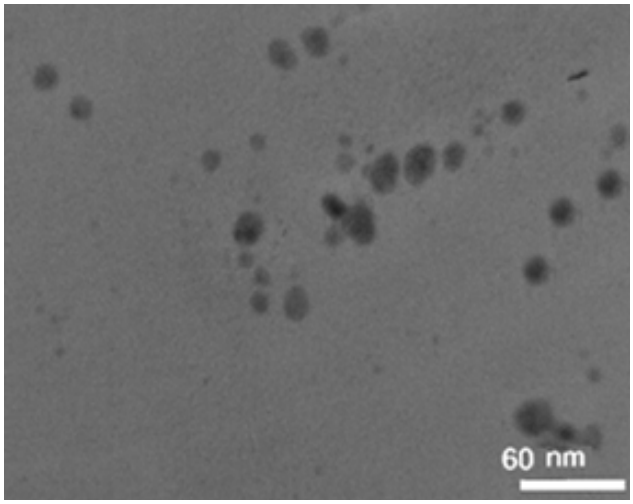


**Figure 1.** The TEM image of the BSA-stabilized gold nanoparticles

### 3.2. Characterization of $Sio_2$@Aunps Nano Composite

The as-synthesized $SiO_2$@AuNPs Nano composite was characterized by the TEM imaging method. In this regard, the TEM image of the as-prepared $SiO_2$@AuNPs Nano composite was recorded using a transmission electron microscope, the results are shown in Figure 2. As shown in this figure the gold nanoparticles were successfully formed on the surface of silica nanoparticles during the synthesis of $SiO_2$@AuNPs Nano composite. According to the TEM image, the as-synthesized $SiO_2$@AuNPs Nano composite has a narrow size distribution of 184.7-217.4 nm. It is notable that the average size of the as-synthesized $SiO_2$@AuNPs Nano composite was calculated at about 204 nm using the TEM imaging method.

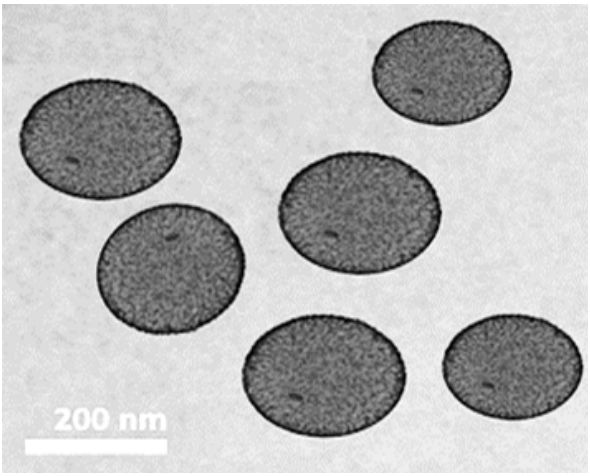


**Figure 2:** The TEM image of the as-synthesized $SiO_2$@AuNPs nanocomposite

### 3.3. Kinetic performances of $SiO_2$@AuNPs Nano composite

Kinetic studies were carried out to calculate the kinetic parameters of the as-prepared $SiO_2$@AuNPs Nano composite toward 2-electron reversible oxidation of TMB. In fact, the kinetic parameters of an enzyme were previously well defined with numeric values including affinity constant ($K_m$) and maximum enzymatic velocity ($A_{max}$) utilizing the Michaelis–Menten steady-state kinetics model. The Vmax value reflects the intrinsic properties of an enzyme or nanozyme and is defined as the highest possible rate of the nanozyme-catalyzed reaction when all enzyme molecules or all nanozyme particles are saturated with the substrate which points to the catalytic efficiency of an enzyme or nanozyme. Hence, the higher value of Amax for an enzymatic/nanozymatic reaction can be assigned to the higher catalytic efficiency of the enzyme or nanozyme [46, 47]. In contrast, the affinity of the substrate of an enzyme or nanozyme for interaction with its active site is represented by the $K_m$, as reported [46]. In fact, the lower values of $K_m$ pointed to the higher affinity of the substrate for binding to the enzyme/nanozyme active site/nodes [17, 40]. Therefore, to quantify the kinetics parameters of the as-prepared $SiO_2$@AuNPs Nano composite, the Michaelis–Menten saturation curve was obtained via plotting the nanozymatic reaction velocity as a function of the substrate (TMB) concertation (Figure 3A). As seen in Figure 3A, the reaction rate of the $SiO_2$@AuNPs nanocomposite-mediated oxidation reaction was increased by increasing the TMB concertation and then reaching a steady-state condition. For accurate estimation of $K_m$ and $V_{max}$ of the $SiO_2$@AuNPs nanocomposite-mediated oxidation reaction, the Line weaver–Burk plot was also constructed for the $SiO_2$@AuNPs nanocomposite-mediated reaction (Figure 3B). The results revealed a Vmax of 0.022 µM min-1 and a $K_m$ as very low as 0.06 mm for the $SiO_2$@AuNPs nanocomposite. Considering the low $K_m$ value of the as-synthesized nanocomposite, it can be concluded that the as-prepared nanocomposite shows high substrate affinity, as reported [17, 41]. Besides, obtaining a $V_{max}$ of 0.022 µM min-1, revealed that the as-prepared nanocomposite has a very good catalytic efficiency.

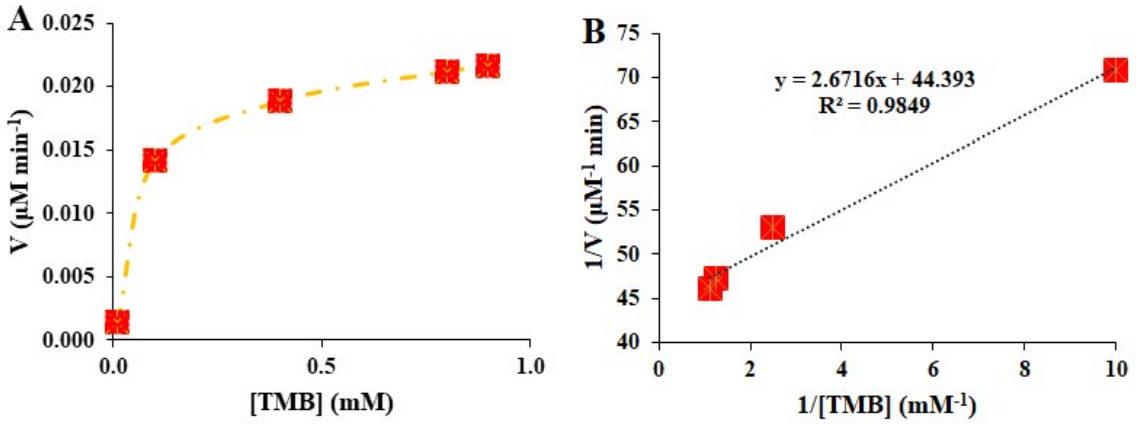


**Figure 3:** (A) Michaelis–Menten curve and (B) Lineweaver–Burk plot for the as-prepared $SiO_2$@AuNPs nanocomposite as peroxidase mimics.

### 3.4. Kinetics performances of BSA-stabilized gold nanoparticles

The kinetics studies for exploring more precise on reporting of the peroxidase-like activity and enzymatic power of the as-prepared BSA-stabilized gold nanozymes were carried out by estimating their activity as a function of substrate concentration and then, the standard Line weaver–Burk plot was provided by plotting the inverse of the velocity of the nanozymatic reaction ($V^{-1}$) as a function of [substrate]-1 for estimating the nanozymatic kinetics parameters. The kinetic parameters of the as-mentioned BSA-stabilized gold nanozymes including $V_{max}$ and $K_m$ were then calculated by plotting the steady-state Michaelis–Menten curve and the linear plot of Line weaver–Burk for both substrates. The Michaelis–Menten plot for the enzymatic oxidation of TMB catalyzed by the as-mentioned BSA-stabilized gold nanozymes was shown in Figure 4A, revealing that the rate of BSA-stabilized gold nanozymes-mediated oxidation of TMB was increased by increasing the substrate concertation and then leveled off. To estimate the kinetic parameters of BSA-stabilized gold nanozymes toward TMB oxidation, the Line weaver–Burk plot was constructed (Figure 4B). Considering the results obtained in Figure 4B, the $V_{max}$ and $K_m$ of the as-mentioned BSA-stabilized gold nanozymes were calculated at about 263 nM $sec^{-1}$ and 0.03 mm, in order.

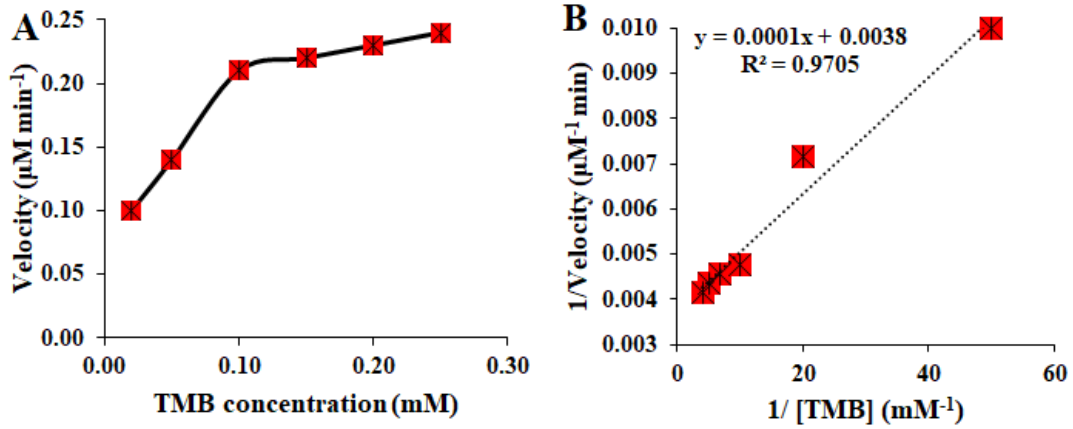


**Figure 4:** Kinetic performances of BSA-stabilized gold nanozymes toward TMB oxidation, (A) Michaelis–Menten plot and (B) Lineweaver–Burk plot.

### 3.5. Kinetics performances of BSA-Stabilized gold nanoparticles vs. $Sio_2$@aunps nanocomposite

The Kinetic parameters of BSA-stabilized gold nanoparticles compared to those of the $SiO_2$@AuNPs nanocomposite toward TMB oxidation are represented in Table 1. As can be seen from this table, the Vmax of BSA-stabilized gold nanoparticles was 12.0-fold higher than that of $SiO_2$@AuNPs nanocomposite, revealing that the catalytic efficiency of BSA-stabilized gold nanoparticles is 12.0-fold higher than $SiO_2$@AuNPs nanocomposite. Besides, the Km value of $SiO_2$@AuNPs nanocomposite was 2-order higher than that of BSA-stabilized gold nanoparticles, indicating that the substrate affinity toward BSA-stabilized gold nanoparticles is 2.0-order higher than the $SiO_2$@AuNPs nanocomposite. Since, the active nodes of both nanozymes are the same (i.e., gold), the difference between their catalytic efficiency and affinity can be assigned to their different sizes and the ability of the active nodes to bind the substrate. Based on the results of this work, small-size BSA-stabilized gold nanoparticles are characteristically more efficient peroxidase mimic materials than the $SiO_2$@AuNPs nanocomposite.

| Nanozyme | Type of active node | Substrate | Size (nm) | $K_m$ (mM) | $V_{max}$ µM $min^{-1}$ |
|---|---|---|---|---|---|
| $SiO_2$@AuNPs nanocomposite | Gold | TMB | 204 | 0.06 | 0.022 |
| BSA-stabilized gold NPs | Gold | TMB | 13 | 0.03 | 0.263 |

**Table 1. Kinetic parameters of BSA-stabilized gold nanoparticles compared to those of the $SiO_2$@AuNPs nanocomposite toward TMB oxidation.**

## 4. Conclusions

In this study, BSA-stabilized gold nanoparticles and $SiO_2$@AuNPs nanocomposite were synthesized and then characterized by the TEM imaging method. The average size of BSA-stabilized gold nanoparticles was found to be as small as 13 nm while the $SiO_2$@AuNPs nanocomposite showed a mean size of 204 nm. The experimental studies revealed that both BSA-stabilized gold nanoparticles and $SiO_2$@AuNPs nanocomposite exhibit intrinsic peroxidase-like activity. Hence, to explore more precise no their catalytic efficiency and substrate affinity, the kinetic characteristics of both nanozymes were quantified using the Menten kinetic model, and the provided results were compared. Upon using TMB as peroxidase substrate, $V_{max}$ of 0.022 µM $min^{-1}$ and a Km of 0.06 mm for the $SiO_2$@AuNPs nanocomposite was achieved while for the BSA-stabilized gold nanoparticles, a $V_{max}$ and $K_m$ at about 0.263 µM $min^{-1}$ and 0.03 mm, in order, was estimated. The Vmax of BSA-stabilized gold nanoparticles was 12.0-fold higher than that of $SiO_2$@AuNPs nanocomposite, revealing that the catalytic efficiency of BSA-stabilized gold nanoparticles is 12.0-fold higher than $SiO_2$@AuNPs nanocomposite. Besides, the Km value of $SiO_2$@AuNPs nanocomposite was 2-order higher than that of BSA-stabilized gold nanoparticles, indicating that the substrate affinity toward BSA-stabilized gold nanoparticles is 2.0-order higher than the $SiO_2$@AuNPs nanocomposite. Since, the active nodes of both nanozymes are same (i.e., gold), the difference between their catalytic efficiency and affinity can be assigned to their different sizes and the ability of the active nodes to bind the substrate. Based on the results of this work, small-size BSA-stabilized gold nanoparticles are characteristically more efficient peroxidase mimic materials than the $SiO_2$@AuNPs nanocomposite.


## Acknowledgments

The authors gratefully thank the Hormozi Laboratory of Chemistry and Biochemistry (Zabol, Iran) for the support of this work.


## Conflict of interest

None.

## References


1. Dehghani, Z., Akhond, M., Jangi, S. R. H., & Absalan, G. (2024). Highly sensitive enantioselective spectrofluorimetric determination of R-/S-mandelic acid using l-tryptophan-modified amino-functional silica-coated N-doped carbon dots as novel high-throughput chiral Nano probes. Talent, 266, 124977.
2. Kelly, K. L., Coronado, E., Zhao, L. L., & Schatz, G. C. (2003). The optical properties of metal nanoparticles: the influence of size, shape, and dielectric environment. The Journal of Physical Chemistry B, 107(3), 668-677.
3. Hormozi Jangi, S. R., & Gholamhosseinzadeh, E. (2023). Developing an ultra-reproducible and ultrasensitive label-free nanoassay for L-methionine quantification in biological samples toward application in homocystinuria diagnosis. Chemical Papers, 1-13.
4. HORMOZI JANGI, S. R., & Akhond, M. (2020). High throughput green reduction of tris (p-nitrophenyl) amine at ambient temperature over homogenous AgNPs as H-transfer catalyst. Journal of Chemical Sciences, 132, 1-8.
5. Hormozi Jangi, S. R. (2023). Low-temperature destructive hydrodechlorination of long-chain chlorinated paraffins to diesel and gasoline range hydrocarbons over a novel low-cost reusable ZSM-5@ Al-MCM nanocatalyst: a new approach toward reuse instead of common mineralization. Chemical Papers, 1-15.
6. Shi, Y., Shan, S., Li, C., Song, X., Zhang, C., Chen, J., ... & Xiong, J. (2020). Application of the tumor site recognizable and dual-responsive nanoparticles for combinational treatment of the drug-resistant colorectal cancer. Pharmaceutical Research, 37, 1-14.
7. Singh, R., & Nalwa, H. S. (2011). Medical applications of nanoparticles in biological imaging, cell labeling, antimicrobial agents, and anticancer Nano drugs. Journal of biomedical nanotechnology, 7(4), 489-503.
8. Rajasekaran, J., & Viswanathan, P. (2023). Anti-bacterial and ant biofilm properties of seaweed polysaccharide-based nanoparticles. Aquaculture International, 1-25.
9. Amany, A., El-Rab, S. F. G., & Gad, F. (2012). Effect of reducing and protecting agents on size of silver nanoparticles and their anti-bacterial activity. Der Pharma Chemica, 4(1), 53-65.
10. Hormozi Jangi, S. R. (2023). Effect of daylight and air oxygen on nanozymatic activity of unmodified silver nanoparticles: Shelf-stability. Qeios. doi, 10.
11. Jangi, S. R. H. (2023). Determining kinetics parameters of bovine serum albumin-protected gold nanozymes toward different substrates. Qeios.
12. Jangi, S. R. H., & Akhond, M. (2021). Ultrasensitive label-free enantioselective quantification of d-/l-leucine enantiomers with a novel detection mechanism using an ultra-small high-quantum yield N-doped CDs prepared by a novel highly fast solvent-free method. Sensors and Actuators B: Chemical, 339, 129901.
13. Li, G., Liu, Z., Gao, W., & Tang, B. (2023). Recent advancement in graphene quantum dots based fluorescent sensor: Design, construction and bio-medical applications. Coordination Chemistry Reviews, 478, 214966.
14. Carapace, A., Martins, M. R., Caldera, A. T., Mario, J., & Dias, L. (2023). Biosynthesis of metal and metal oxide nanoparticles using microbial cultures: Mechanisms, antimicrobial activity and applications to cultural heritage.

Microorganisms, 11(2), 378.
15. Dongsar, T. T., Dongsar, T. S., Abourehab, M. A., Gupta, N., & Kesharwani, P. (2023). Emerging application of magnetic nanoparticles for breast cancer therapy. European Polymer Journal, 111898.
16. Jangi, S. R. H., & Akhond, M. (2021). High throughput urease immobilization onto a new metal-organic framework called nanosized electroactive quasi-coral-340 (NEQC-340) for water treatment and safe blood cleaning. Process Biochemistry, 105, 79-90.
17. Hormozi Jangi, S. R. (2023). Synthesis and characterization of magnesium-based metal-organic frameworks and investigating the effect of coordination solvent on their biocompatibility. Chemical Research and Nanomaterials, 1(4), 1-9.
18. Li, W., Chen, B., Zhang, H., Sun, Y., Wang, J., Zhang, J., & Fu, Y. (2015). BSA-stabilized Pt nanozyme for peroxidase mimetics and its application on colorimetric detection of mercury (II) ions. Biosensors and Bioelectronics, 66, 251-258.
19. Jangi, A. R. H., Jangi, M. R. H., & Jangi, S. R. H. (2020). Detection mechanism and classification of design principles of peroxidase mimic based colorimetric sensors: A brief overview. Chinese Journal of Chemical Engineering, 28(6), 1492-1503.
20. Hormozi Jangi, S. R., & Dehghani, Z. (2023). Spectrophotometric quantification of hydrogen peroxide utilizing silver nanozyme. Chemical Research and Nanomaterials, 2(1), 15-23.
21. Jangi, S. R. H. (2023). Introducing a high throughput nanozymatic method for eco-friendly nanozyme-mediated degradation of methylene blue in real water media. Sustainable Chemical Engineering, 90-99.
22. Huang, Y., Ran, J., & Qu, X. (2019). Nanozymes: classification, catalytic mechanisms, activity regulation, and applications. Chemical reviews, 119(6), 4357-4412.
23. Lu, L., Huang, M., Huang, Y., Corvini, P. F. X., Ji, R., & Zhao, L. (2020). Mn 3 O 4 nanozymes boost endogenous antioxidant metabolites in cucumber (Cucumis sativus) plant and enhance resistance to salinity stress. Environmental Science: Nano, 7(6), 1692-1703.
24. Xia, F., Shi, Q., & Nan, Z. (2020). Facile synthesis of Cu-Cafes 2 O 4 nanozymes for sensitive assay of H 2 O 2 and GSH. Dalton Transactions, 49(36), 12780-12792.
25. Liu, J., GAO, J., Zhang, A., Guo, Y., Fan, S., He, Y. ... & Cheng, Y. (2020). Carbon Nano cage-based nanozyme as an endogenous H 2 O 2-activated oxygenator for real-time bimodal imaging and enhanced phototherapy of esophageal cancer. Nano scale, 12(42), 21674-21686.
26. Dega, N. K., Ganganboina, A. B., Tran, H. L., Kuncoro, E. P., & Doing, R. A. (2022). BSA-stabilized manganese phosphate Nano flower with enhanced nanozyme activity for highly sensitive and rapid detection of glutathione. Talent, 237, 122957.
27. Sun, H., Zhou, Y., Ren, J., & Qu, X. (2018). Carbon nanozymes: enzymatic properties, catalytic mechanism, and applications. Angewandte Chemie International Edition, 57(30), 9224-9237.
28. Jangi, S. R. H., Davoudli, H. K., Delshad, Y., Jangi, M. R. H., & Jangi, A. R. H. (2020). A novel and reusable multinanozyme system for sensitive and selective quantification of hydrogen peroxide and highly efficient degradation of organic dye. Surfaces and Interfaces, 21, 100771.
29. Hormozi Jangi, S. R., Akhond, M., & Absalan, G. (2020). A field-applicable colorimetric assay for notorious explosive triacetone triperoxide through nanozyme-catalyzed irreversible oxidation of 3, 3′-diaminobenzidine. Microchimica Acta, 187, 1-10.
30. Dong, H., Du, W., Dong, J., Che, R., Kong, F., Cheng, W., ... & Zhang, Y. (2022). Depletable peroxidase-like activity of Fe3O4 nanozymes accompanied with separate migration of electrons and iron ions. Nature Communications, 13(1), 5365.
31. Meng, X., Li, D., Chen, L., He, H., Wang, Q., Hong, C., ... & Fan, K. (2021). High-performance self-cascade pyrite nanozymes for apoptosis–ferroptosis synergistic tumor therapy. ACS nano, 15(3), 5735-5751.
32. Jangi, S. R. H., & Akhond, M. (2020). Synthesis and characterization of a novel metal-organic framework called nanosized electroactive quasi-coral-340 (NEQC-340) and its application for constructing a reusable nanozyme-based sensor for selective and sensitive glutathione quantification. Microchemical Journal, 158, 105328.
33. Jangi, S. R. H., Akhond, M., & Absalan, G. (2020). A novel selective and sensitive multinanozyme colorimetric method for glutathione detection by using an indamine polymer. Analytica Chimica Acta, 1127, 1-8.
34. Chen, Y., Jiao, L., Yan, H., Xu, W., Wu, Y., Wang, H., ... & Zhu, C. (2020). Hierarchically porous S/N codoped carbon nanozymes with enhanced peroxidase-like activity for total antioxidant capacity biosensing. Analytical Chemistry, 92(19), 13518-13524.
35. Hormozi Jangi, S. R., & Dehghani, Z. (2023). Kinetics and biochemical characterization of silver nanozymes and investigating impact of storage conditions on their activity and shelf-life. Chemical Research and Nanomaterials, 1(4), 25-33.
36. Zhou, X., Wang, M., Chen, J., & Su, X. (2022). Cascade reaction biosensor based on Cu/N co-doped two-dimensional carbon-based nanozyme for the detection of lactose and β-galactosidase. Talanta, 245, 123451.
37. Akhond, M., Hormozi Jangi, S. R., Barzegar, S., & Absalan, G. (2020). Introducing a nanozyme-based sensor for selective and sensitive detection of mercury (II) using its inhibiting effect on production of an indamine polymer through a stable n-electron irreversible system. Chemical Papers, 74, 1321-1330.
38. Zeng, X., Ruan, Y., Chen, Q., Yan, S., & Huang, W. (2023). Biocatalytic cascade in tumor microenvironment with a Fe2O3/Au hybrid nanozyme for synergistic treatment of triple negative breast cancer. Chemical Engineering Journal, 452, 138422.
39. Ahmadi-Leilakouhi, B., Hormozi Jangi, S. R., & Khorshidi, A. (2023). Introducing a novel photo-induced nanozymatic method for high throughput reusable biodegradation of

organic dyes. Chemical Papers, 77(2), 1033-1046.
40. Jangi, S. R. H. (2023). Natural Polyphenols of Pomegranate and Black Tea Juices can Combat COVID-19 through their SARS-CoV-2 3C-like Protease-inhibitory Activity. Qeios.
41. Hormozi Jangi, S. R. (2023). A Brief Overview on Clinical and Epidemiological Features, Mechanism of Action, and Diagnosis of Novel Global Pandemic Infectious Disease, Covid-19, And its Comparison with Sars, Mers, And H1n1. World J Clin Med Img, 2(1), 45-52.
42. Meng, X., Zou, S., Li, D., He, J., Fang, L., Wang, H., ... & Gao, L. (2022). Nanozyme-strip for rapid and ultrasensitive nucleic acid detection of SARS-CoV-2. Biosensors and Bioelectronics, 217, 114739.
43. Hormozi Jangi, S. R. (2023). Biochemical characterization of enzyme-like silver nanoparticles toward nanozyme-catalysed oxidation reactions. Micromaterials and Interfaces, 1(1), 2170.
44. Jangi, S. R. H. (2023). A Comparative Study on Kinetics Performances of BSA-gold Nanozymes for Nanozyme-Mediated Oxidation of 3, 3', 5, 5'-Tetramethylbenzidine and 3, 3'-Diaminobenzidine.
45. Hormozi Jangi, S. R. (2023). Evaluation of Biochemical Behavior and Stability of Gold Nanoparticles with High Intrinsic Peroxidase-Like Activity. Petro Chem Indus Intern, 6(4), 234-239.
46. Jangi, S. R. H., Akhond, M., & Dehghani, Z. (2020). High throughput covalent immobilization process for improvement of shelf-life, operational cycles, relative activity in organic media and enzymatic kinetics of urease and its application for urea removal from water samples. Process Biochemistry, 90, 102-112.
47. Jangi, S. R. H., & Akhond, M. (2022). Introducing a covalent thiol-based protected immobilized acetylcholinesterase with enhanced enzymatic performances for biosynthesis of esters. Process Biochemistry, 120, 138-155.